The electrocrystallization of zinc from alkaline media

The Electrocrystallization of Zinc from Alkaline Media

M. Y. Abyaneh, J. Hendrikx, W. Visscher, and E. Barendrecht*

Eindhoven University of Technology, Laboratory for Electrochemistry, 5600 MB Eindhoven, The Netherlands

ABSTRACT

The initial stages of the electrocrystallization of zinc from an alkaline electrolyte onto a polycrystalline silver substrate are investigated using the potential step method. In the overpotential region where the reaction is predominantly controlled by charge transfer, computer analysis of the experimental current-time transients with detailed models of nucleation and growth is possible. This gives information about the kinetics of the reaction and the morphology of the crystal growth. It is concluded that the electrocrystallization of zinc proceeds via nucleation and growth, first of a thin layer of primary centers, having low angle of contact at low overpotentials, and subsequently by a layer, which starts to grow via secondary centers, formed at the sites where the primary centers coalesce.

The electrocrystallization of zinc has been extensively studied from the technological point of view. The number of publications on this subject is continuously increasing due to the promising features of zinc as electrode material in rechargeable batteries. The complexity of the behavior of this metal as an electrode is evident from different types of studies and contradictory data found in the literature. Only few investigations [see for example references (1, 2)] have been carried out on the first stages of the deposition of zinc. However, these studies still lack the detailed analysis of the very initial stages such as the initial formation of monolayers and the initial nucleation and three-dimensional growth of centers.

It is now well established (3) that detailed information about the kinetics of electrocrystallization can be obtained readily from the initial stages of the potentiostatic deposition on foreign substrates. The electrocrystallization of nickel, an irreversible process, was recently examined (4) by this technique and it was shown that the computer-based analysis of the initial stages of the deposition (5), according to the relevant general electrocrystallization models (6), gives direct information as to the kinetics of nucleation, the kinetics of crystal growth in two and three dimensions, the morphology of the deposit, and the role of "overlap" of growth centers, etc.

The main aim of the work reported here is to explore the extent to which such studies can be used to derive similar information about a reversible process, the electrocrystallization of zinc.

Theory

Derivation of current-time equations for electrocrystallization processes requires as a prerequisite the correct calculation of the actual area of growth centers at any time, t, prior to and after the coalescence of centers. It was pointed out recently (7, 8) that the statistical treatments of overlap (9) used for such calculations account for all ingestion of sites due to their coverage by the growth processes, but ingestion of sites due to the conversion of sites into nuclei are not accounted for; this type of ingestion must then be taken into consideration by introducing a nucleation law (7, 8)

$$N = \frac{A}{A'}(1 - \exp - A't) \qquad [1]$$

where A (nuclei cm^{-2} sec^{-1}) is the initial rate of nucleation, A' (sec^{-1}) is the rate of conversion of a site into a nucleus, and N (nuclei cm^{-2}) is the total number of nuclei that can be formed in time t in the absence of growth processes. If nucleation is progressive in time and occurs at only N_0 (cm^{-2}) preferred sites, then the total number of nuclei that can be formed in the absence of growth is given by

$$\frac{A}{A'} = N_0 \qquad [2]$$

whereas for the case of progressive nucleation in the absence of such preferred sites

$$\frac{A}{A'} = \frac{1}{\alpha r_c^2} \qquad [3]$$

where r_c (cm) is the critical size of a nucleus and α is a packing factor.

General current-time equations for nucleation and two-dimensional growth of centers together with the concurrent hydrogen evolution (6) give rise to a transient shown in Fig. 1. The initial current in this case rises with time according to

$$i \sim t^n \qquad [4]$$

where $2 \geq n \geq 1$ depending on whether A' is very large ($n = 1$ for $A' = \infty$) or very small ($n = 2$ for A' very small compared to the overall rate of the process). The steady-state current is due to hydrogen evolution on top of the monolayer deposit.

The general current-time equation for nucleation and three-dimensional growth of centers whose shapes are approximated by right-circular cones, Fig. 2A, is given by (6)

$$i = zFk'\left\{1 - \exp\left[\frac{-\pi M^2 k^2 A}{A'\rho^2}\left(t^2 - \frac{2t}{A'} + \frac{2}{A'^2} - \frac{2}{A'^2}\exp(-A't)\right)\right]\right\} \qquad [5]$$

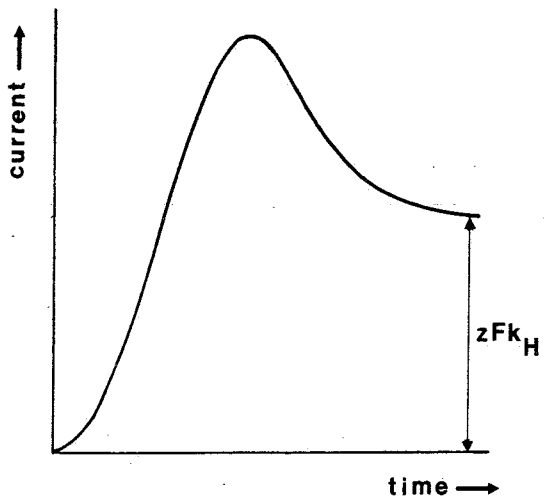

Fig. 1. Theoretical current-time transient due to the two-dimensional nucleation and growth together with evolution of hydrogen (on the tops and at the edges of the growth centers).

* Electrochemical Society Active Member.
Key words: initial, deposition, zinc, alkaline media.

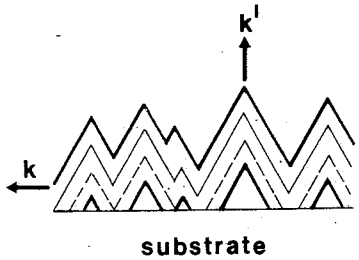

Fig. 2A. Growth of right-circular cones, viewed at four different times.

where k' (mols cm^{-2} sec^{-1}) and k (mols cm^{-2} sec^{-1}) are the rates of crystal growth in the direction perpendicular and parallel to the substrate, and M (g mol^{-1}) and ρ (g cm^{-3}) are the molecular weight and the density of the deposit, respectively.

Equation [5] has two limiting forms. If the nucleation is instantaneous (*i.e.*, $A' = \infty$; $N = A/A' = N_0$), the current-time equation is given by

$$i = zFk' \left\{ 1 - \exp \frac{-\pi M^2 k^2 N_0}{\rho^2} t^2 \right\} \qquad [6]$$

If the nucleation is progressive and $1/A'$ is large compared to the overall time, the current-time equation is given by

$$i = zFk' \left\{ 1 - \exp \frac{-\pi M^2 k^2 A}{3\rho^2} t^3 \right\} \qquad [7]$$

The above Eq. [5], [6], and [7] predict an asymptotic approach of current to a constant value, zFk' (A cm^{-2}), Fig. 2B. However, the transients for the deposition of nickel (4, 5) and cobalt (10) on a vitreous carbon electrode show that the current goes through a maximum. The appearance of this maximum current in the initial stages of the potentiostatic deposition of nickel has been explained by the mechanism of "death" and synchronized "rebirth" (5) of new centers: a mechanism also observed (11) by electron microscopic studies of the initial stages of the deposition of nickel onto {111} single crystal copper.

It has recently been shown (12) that nucleation, growth, and overlap of hemispherical centers, also considered later in this paper, can adequately explain the transients of the electrocrystallization of nickel without further assumptions of death and rebirth processes.

Experimental

The electrocrystallization of zinc was studied on silver electrodes in alkaline zincate solutions. Measurements were made in a conventional three-compartment cell at 295 ± 1 K, using a Wenking potentiostat (68 FR.5) and a Universal Programmer (PAR 175); the current-time transients were recorded on a Kipp (BD8 multirange) chart recorder. The reference electrode is an Hg/HgO electrode and all potentials are given with respect to this electrode. The counterelectrode is a high purity zinc rod.

A polycrystalline silver rod electrode of purity 99.95% and 6 mm in diameter, embedded in KelF was polished with successively finer grades of alumina (down to 0.05 μm); the electrode was then cleaned by pouring first fast running tap water and then doubly distilled water over it. The experimental work was carried out in 10M KOH + 0.5M ZnO solutions prepared from AnalaR Chemicals and doubly distilled water. The solutions were freshly prepared prior to each set of experiments.

The Ag electrode, in each experiment, was inserted into the cell at 0.0V; the potential was then stepped to the value E_r (which was previously determined as being the rest potential of a pure zinc rod in the solution in use) for a period long enough for the background current to fall to a steady low value. Next, a further step to the appropriate working potential was applied so as to initiate the electrocrystallization of zinc. The overpotentials, here defined as the difference $E - E_r$, were varied between 24 and 35 mV.

Results

General features of the initial stages of the electrodeposition of zinc.—Figure 3 illustrates the initial part of the current-time transient observed for the potentiostatic deposition of zinc onto a polycrystalline silver electrode at a potential of − 1.381V (E_r = −1.355V). In the time range $0 < t < t_1$ the deposition of a layer can be observed (peak A).

At $t > t_1$ nucleation and three-dimensional growth of centers take place. The growth of these centers in the direction parallel to the substrate is impeded by their coalescence during the later stages. The current goes through a maximum at $t = t_2$ (peak B) and decreases rather slowly compared to the rising portion of the transient. Figure 4 shows the longer time features of the transient shown in Fig. 3. It can be seen that the current after falling to a relatively low value at $t = t_3$ slowly rises again, indicating the rebirth of new centers on the top of the underlying deposit and their subsequent growth into the solution. Successive increase in overpotential drastically decreases the time scale and increases the current scale at which peaks A and B occur (see Fig. 5 at $E = -1.385$V and Fig. 6 at $E = -1.390$V). Overlap of the two transients (one observed at $t < t_1$ and the other at $t > t_1$, Fig. 3)

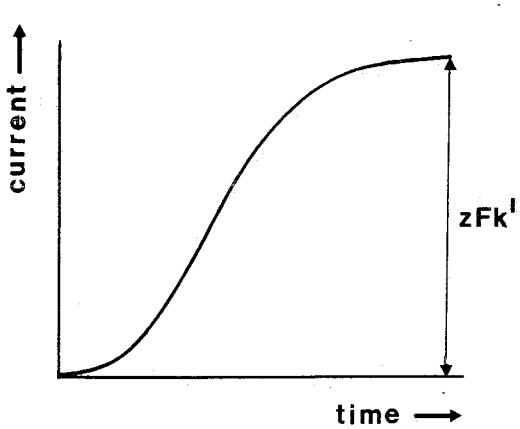

Fig. 2B. Current-time transient according to Eq. [5]

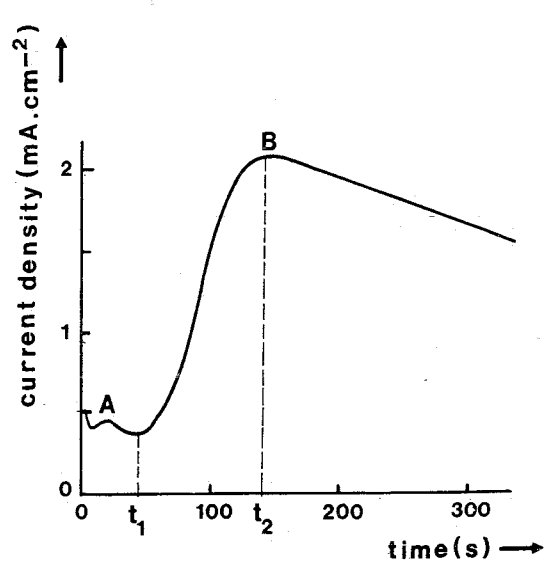

Fig. 3. Initial part of the current-time transient of the deposition of zinc onto a polycrystalline silver electrode at −1.381V (vs. Hg/HgO).

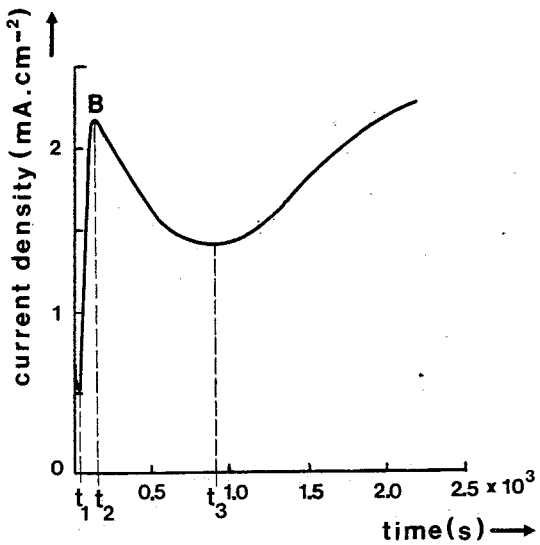

Fig. 4. The extended longer time part of the transient shown in Fig. 3.

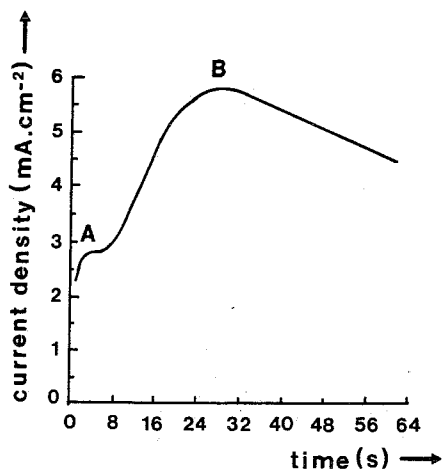

Fig. 5. Initial part of the current-time transient of the deposition of zinc onto a polycrystalline silver electrode at —1.385V (vs. Hg/HgO).

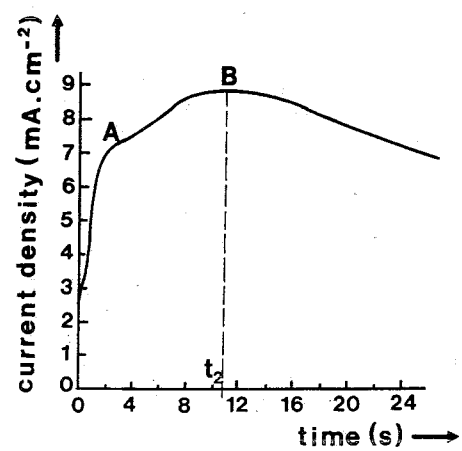

Fig. 6. Initial part of the current-time transient of the deposition of zinc onto a polycrystalline silver electrode at —1.390V (vs. Hg/HgO).

and a larger increase of the current peak A, with respect to that of B, is also observed.

Detailed analysis of the initial stages.—The formation of the layer of deposit observed in the time range $0 < t < t_1$ (Fig. 3) is by no means the first layer formed on a silver substrate. Potential sweep measurements (Fig. 7) show, at cathodic potentials smaller than that of Fig. 3, monolayer/adsorption peaks prior to the formation of this layer, as also found in Ref. (13). The relatively large, diminishing background current observed in Fig. 3 at the very beginning of the transient is thus mostly due to fast formation of these initial layers which, however, are not investigated in this paper. If the layer, observed in the above time range is assumed to be formed via a two-dimensional nucleation and growth process with concurrent evolution of hydrogen at the edges and on the tops of the growth centers, then at time t_1 (when the monolayer formation is completed) the current is given by

$$i_H = zFk_H \qquad [8]$$

where k_H (mols cm^{-2} sec^{-1}) is the rate constant for the evolution of hydrogen on the top surface of the full layer. The nucleation and three-dimensional growth of centers must then take place on the top of this already deposited layer. Assuming right-circular cone growth forms, the total current-time equation describing the transient, in the time range $t_1 < t < t_2$, is given by Eq. [5] and [8]

$$i = i_H + zFk'\left\{1 - \exp\left[-\frac{\pi M^2k^2A}{A'\rho^2}\left((t-t_1)^2 - \frac{2(t-t_1)}{A'} + \frac{2}{A'^2} - \frac{2}{A'^2}\exp - A'(t-t_1)\right)\right]\right\} \qquad [9]$$

provided that there are no other processes, such as the death and rebirth of crystal growth. Figure 8 is the computer fit of the experimental transient, Fig. 3, in the above time range to this equation. It is worthwhile to note that the nucleation rate constant A' (sec^{-1}) is directly obtained by this computer fit.

A computer fit of the same experimental data of Fig. 3 in this time range, $t_1 < t < t_2$, to the simplified form of Eq. [9] for progressive nucleation (Eq. [7] + [8]), shows that the fit is slightly less than in Fig. 8 (standard error of fit: 0.17 10^{-1} mA cm^{-2}), indicating that Eq. [7] is indeed only an approximation of the general relation (Eq. [5]).

The current-time transients obtained at higher potentials [$E = -1.385$V (Fig. 5); $E = -1.390$V (Fig. 6)] show that here, evidently, the mechanism of two-dimensional nucleation and growth can no longer be an adequate description of the first transient peak. Indeed, when these transient data are fitted to the current-time equations (describing monolayer formations

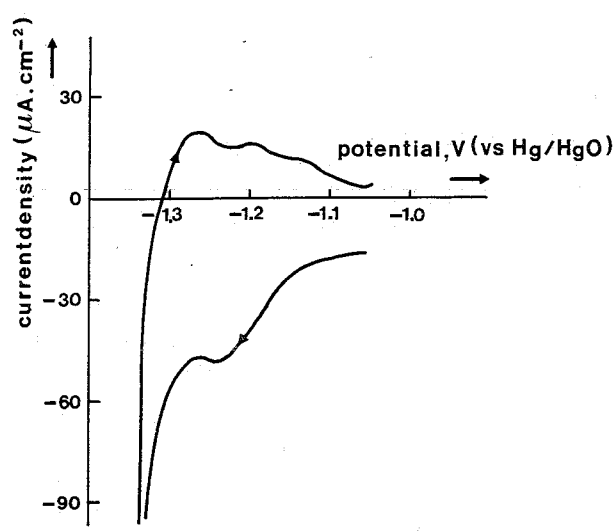

Fig. 7. Cyclic voltammogram of a polycrystalline silver electrode in 10M KOH + 0.5M ZnO; sweep rate: 10 mV/sec; first sweep, after polishing, between 0 and —1.33V.

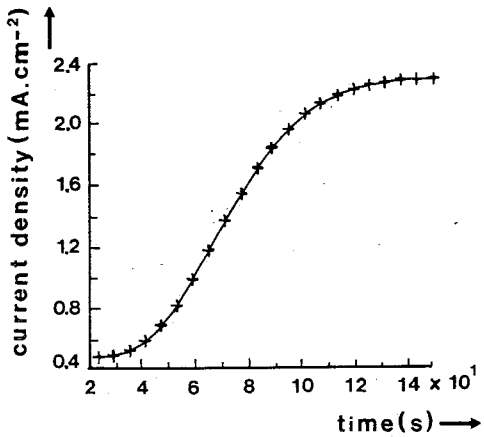

Fig. 8. The part of the current-time transient shown in Fig. 3 in the time range $t_1 < t < t_2$. ++: Experimental data; ——: theoretical fit of Eq. [9]. Derived parameters: $i_H = 0.479 \pm 0.003$ (mA cm^{-2}), $k' = (0.931 \pm 0.002)\ 10^{-8}$ (mols cm^{-2} sec^{-1}), $k^2A/A' = (0.161 \pm 0.003)\ 10^{-6}$ (mols cm^{-6} sec^{-2}), $A' = 0.11 \pm 0.02$ (sec^{-1}), $t_1 = 24.3 \pm 0.8$ (sec). Standard error of fit: 0.36 10^{-2} (mA cm^{-2}).

simultaneously with nucleation and three-dimensional growth of centers on the top of the two-dimensional growth centers), large negative values for the evolution of hydrogen and negative rate constants are obtained; *i.e.*, this model is no longer operative.

In order to explain the current-time behavior at higher potentials we propose a model in which nucleation and three-dimensional growth of primary centers, having low contact angle, θ, (Fig. 9) at low overpotential, are followed by nucleation of secondary three-dimensional growth centers at the junctions where coalescence of the primary centers occurs. We assume in this model that the nucleation is instantaneous. The derivation of the current-time equation for this model is straightforward. The current, i_p, due to the instantaneous nucleation and three-dimensional growth of primary centers is given by Eq. [6] in the following notation

$$i_p = zFk_p' \left(1 - \exp \frac{-\pi M^2 k_p^2 N_0 t^2}{\rho^2}\right) \qquad [10]$$

where subscript p denotes that the rates belong to the nucleation and growth of primary centers. After an induction time, t_1, growth of secondary centers starts at junctions where primary centers have coalesced. The growth of secondary centers affects the total current in two ways, first by decreasing the current (due to the decrease in the actual area of the primary centers) by an amount of

$$i_{-p} = zFk_p' \left(1 - \exp \frac{-\pi M^2 k_s^2 N_0}{\rho^2} (t - t_1)^2\right) \qquad [11]$$

and second by increasing the current by

$$i_s = zFk_s' \left(1 - \exp \frac{-\pi M^2 k_s^2 N_0}{\rho^2} (t - t_1)^2\right) \qquad [12]$$

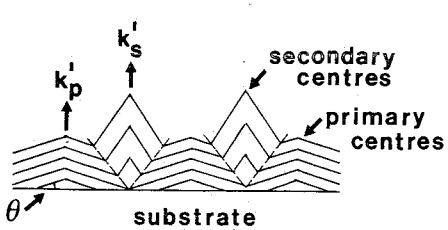

Fig. 9. Growth of secondary right-circular cone centers at sites where primary centers coalesce. θ = contact angle of the primary centers.

where subscript s refers to the secondary centers. A complete decription of the transient, Fig. 5 and 6, up to the second maximum must, moreover, also include the initial diminishing background current. If we assume that the fall in the background current, i_b, is related to the coverage of the primary growth centers, then

$$i_b = i_b' \exp \left(\frac{-\pi M^2 k_p^2 N_0 t^2}{\rho^2}\right) \qquad [13]$$

where i_b' is the value of current observed at $t = 0$.

The total current is then given by

$$i = i_b + i_p \text{ for } t \leq t_1 \qquad [14]$$

and by

$$i = i_b + i_p - i_{-p} + i_s \text{ for } t \geq t_1 \qquad [15]$$

Figures 10 and 11 show the computer fit of the experimental transients at potentials of −1.385 and −1.390V to the above Eq. [14] and [15]. In Fig. 12, k_s', the growth rate constant of the secondary centers in the direction perpendicular to the substrate is plotted against the overpotential. In this small potential region a nearly linear relation is obtained, indicating that the linearized form of the Butler-Volmer relation is valid

$$i = zFk_s' = i_o \frac{zF\eta}{RT} \qquad [16]$$

in which i_o is the exchange current density. The calculated i_o value is about 100 A/m^2 (related to the geometric area of the electrode). In the literature (14-16) i_o values of 200-3100 A/m^2 are given. It is a moot question whether this i_o value can be compared with the i_o values for the Zn → Zn^{2+} reaction, as determined in the literature. The growth of the secondary centers starts after an induction period (t_1) which decreases at higher overpotentials.

The reproducibility of the derived parameters is good, if we take into account the variation in the surface of the silver substrate for each experiment and the sensitivity of the different parameters on the overvoltage. The transient according to Eq. [15] and [9], however, deviates from the experimental data at longer times as Eq. [15] and [9] predict an asymptotic approach of current to a constant value. This is discussed later on.

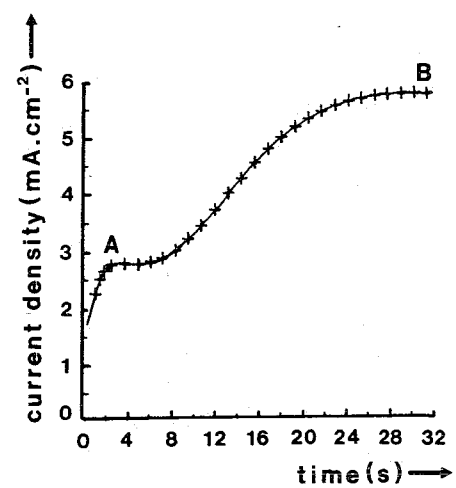

Fig. 10. (Initial) current-time transient of the deposition of zinc onto a polycrystalline silver electrode at −1.385V (vs. Hg/HgO). ++: Experimental data; ——: theoretical fit of Eq. [14] and [15]. Derived parameters: $i_b' = 1.69 \pm 0.04$ (mA cm^{-2}), $k_p' = (0.1429 \pm 0.0002)\ 10^{-7}$ (mols cm^{-2} sec^{-1}), $k_p^2N_0 = (0.22 \pm 0.01)\ 10^{-2}$ (mols^2 cm^{-6} sec^{-2}), $k_s' = (0.2973 \pm 0.0002)\ 10^{-7}$ (mols cm^{-2} sec^{-1}), $k_s^2N_0 = (0.309 \pm 0.003)\ 10^{-4}$ (mols cm^{-6} sec^{-2}), $t_1 = 5.26 \pm 0.03$ (sec). Standard error of fit: 0.68 10^{-2} mA cm^{-2}.

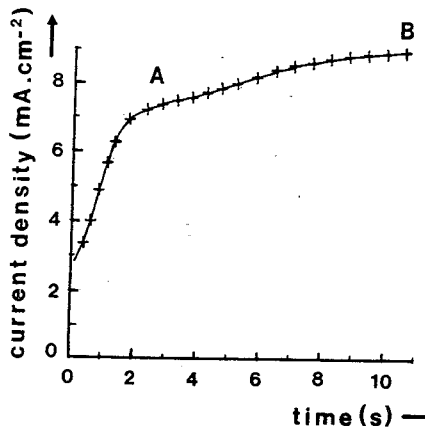

Fig. 11. Initial current-time transient of the deposition of zinc onto a polycrystalline silver electrode at −1.390V (vs. Hg/HgO). ++: Experimental data; ——: theoretical fit of Eq. [14] and [15]. Derived parameters: $i_b' = 2.78 \pm 0.03$ (mA cm^{-2}), $k_p' = (0.375 \pm 0.002)\ 10^{-7}$ (mols cm^{-2} sec^{-1}), $k_p^2N_0 = (0.30 \pm 0.01)\ 10^{-2}$ (mols^2 cm^{-6} sec^{-2}), $k_s' = (0.465 \pm 0.002)\ 10^{-7}$ (mols^2 cm^{-2} sec^{-1}), $k_s^2N_0 = (0.16 \pm 0.02)\ 10^{-3}$ (mols^2 cm^{-6} sec^{-2}), $t_1 = 1.5 \pm 0.2$ (sec). Standard error of fit: 0.25 10^{-2} mA cm^{-2}).

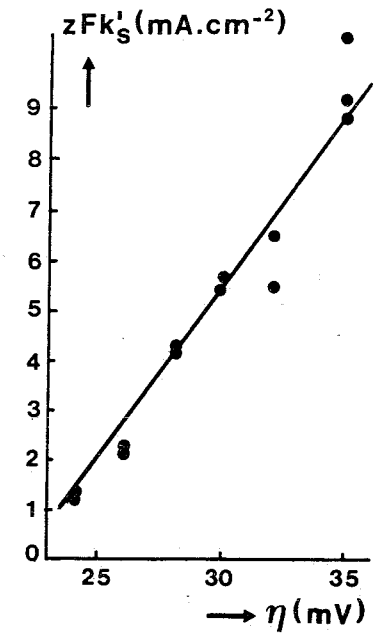

Fig. 12. Plot of zFk_s' against η. k_s' = rate of growth of the secondary centers in the direction perpendicular to the substrate, as obtained by curve fitting.

Experimentally the current increases again after a decrease beyond point B, resulting in a minimum at $t = t_3$ (Fig. 4). On fitting the equations for nucleation and three-dimensional growth of centers to the transient, Fig. 4, at $t > t_3$, a good fit is obtained, indicating that the deposit in this range is again formed via the nucleation and 3-dimensional growth. This deposit appeared to be mossy.

Discussion

The transient behavior of nucleation and growth of conical forms were considered in the theoretical section. The initial transient current is governed mainly by factors that affect the coverage of the substrate, such as the shape of the basal plane of the growth centers and the operative nucleation and growth laws. The actual topography of the centers exerts influence after their coalescence and becomes the dominating factor for the transient shape after the full coverage. The very good fit of the transients for zinc to the equations indicates that the nucleation and three-dimensional growth of centers are indeed responsible for the initial stages. We note that models based on right-circular cone growth forms predict an asymptotic approach of current to a steady-state value and further assumptions about the cessation of growth above and over that due to the coalescence are necessary. Furthermore, the current-time transients over a range of overpotentials were explained by two models, one at low (Fig. 3) and the other at higher overpotentials (Fig. 5 and 6). We like to point out that the above models can be replaced by only one model in which no further assumptions are needed. In this model (Fig. 13) spherical-cap growth centers instead of right-circular cones are considered. Whereas continued growth of the conical centers following overlap preserves the topography of the surface, Fig. 2A (so that the current approaches a limit, Fig. 2B), the continued growth of spherical cap centers leads to a smoothing of the surface, Fig. 14A (with hemispherical caps). The current-time equation based on nucleation law (1) for the growth of such centers is complicated; here we only consider the current-time equations developed (12) for the nucleation and growth of hemispherical centers ($\theta = \pi/2$ in Fig. 14A) based on the two limiting cases of (*i*) instantaneous conversion of N_0 (cm^{-2}) sites into nuclei, for which the current is given by

$$i \simeq \frac{2z\mathbf{F}\pi M^2k^3N_0t}{\rho^2} \exp\left(-\frac{\pi M^2k^2N_0t^2}{\rho^2}\right) \int_0^t \exp\frac{\pi M^2k^2N_0u^2}{\rho^2}\,du \quad [17]$$

and (*ii*) progressive nucleation when $1/A'$ is large compared to the overall time of growth for which

$$i \simeq \frac{z\mathbf{F}\pi M^2k^3A}{\rho^2} \exp\left(-\frac{\pi M^2k^2At^3}{3\rho^2}\right) \int_0^t (t^2 - u^2) \exp\frac{-\pi M^2k^2A}{3\rho^2}(2u^3 - 3tu^2)\,du \quad [18]$$

Both these equations predict a maximum in the current-time behavior, Fig. 14B, except that Eq. [17] predicts an initial current rise proportional to the square of time whereas Eq. [18] indicates an initial rise proportional to the cube of time; both transients reach a steady-state value of $z\mathbf{F}k$ at extended times. However, the correlation between experimental data and theoretical equations is not yet made.

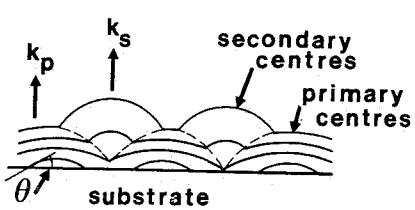

Fig. 13. Growth of secondary hemispherical centers at sites where the primary centers coalesce.

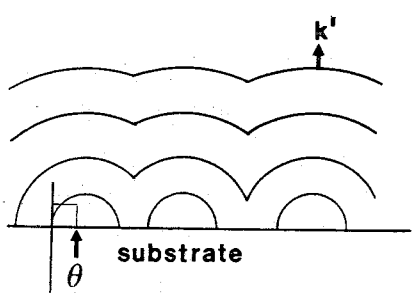

Fig. 14A. Growth of hemispherical cap centers viewed at four different times.

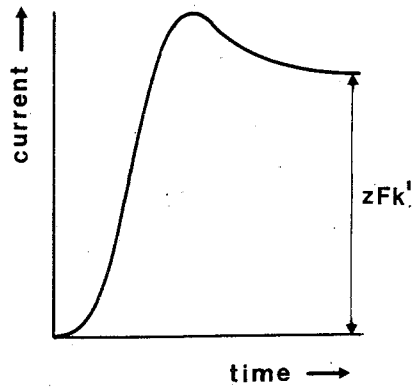

Fig. 14B. Theoretical current-time transient for the mechanism of crystal growth, illustrated in Fig. 14A.

In order to find out whether the peak currents observed in Fig. 3, 5, and 6 are due to any transport processes, the deposition of zinc onto a rotating Ag disk electrode is studied.

The current-time transient (Fig. 15) of the potentiostatic deposition of zinc onto a rotating disk electrode also shows the presence of peak currents, indicating that these currents are indeed caused by the decrease of the area of the deposit after coalescence.

In practice zinc is deposited at high rates where the reaction is predominantly controlled by the diffusion of species through the solution. Here we have only studied the deposition at low rates, *i.e.*, at low overpotentials, as the detailed information about the nucleation and growth mechanism can be easily followed and understood under these conditions. Further insight into the complexity of the behavior of zinc is clearly required for a variety of experimental conditions.

Conclusions

Measured *i-t* transients for electrodeposition of zinc from an alkaline medium onto a silver substrate were compared with calculated transients for models of crystal nucleation and growth.

The electrocrystallization of zinc is found to go through the following stages:

1. Adsorption/underpotential monolayer formation of zinc followed by:

2. The formation of a thin layer by nucleation and three-dimensional growth of primary centers, with a low contact angle at low overpotential (24 mV) and an increase in this contact angle at higher overpotential.

3. The formation of a second layer by nucleation and 3-dimensional growth of secondary centers, at low overpotential on the top of the first layer and at higher overpotential at the junctions where the primary centers coalesce. The primary and secondary nucleation and crystal growth lead to the formation of a compact deposit, prior to:

4. Nucleation and three-dimensional growth of centers leading to the formation of a loose mossy deposit.

Acknowledgment

The authors would like to thank the Netherlands Organization for the Advancement of Pure Research (Z.W.O.) and the NIVEE Foundation for the financial support, and one of us (M.Y.A.) also the Eindhoven University of Technology for the fellowship.

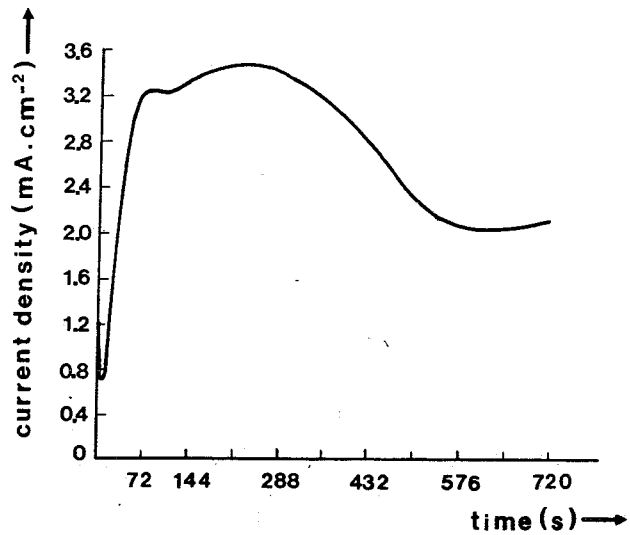

Fig. 15. Current-time transient of the deposition of zinc onto a rotating (2000 rpm) polycrystalline silver electrode at −1.382V (vs. Hg/HgO).

Manuscript submitted Feb. 16, 1982; revised manuscript received *ca.* April 30, 1982.

Any discussion of this paper will appear in a Discussion Section to be published in the June 1983 JOURNAL. All discussions for the June 1983 Discussion Section should be submitted by Feb. 1, 1983.

Publication costs of this article were assisted by The Eindhoven University of Technology.

REFERENCES

1. F. Mansfeld and S. Gilman, *This Journal*, **117**, 588 (1970).
2. A. R. Despic, in "Proceedings of the Third Symposium on Electrode Processes," S. Bruckenstein, J. D. E. McIntyre, B. Miller, and E. Yeager, Editors, p. 235, The Electrochemical Society Softbound Proceedings Series, Princeton, NJ (1979).
3. M. Fleischmann and H. R. Thirsk, in "Advances in Electrochemistry and Electrochemical Engineering," Vol. III, P. Delahay and C. W. Tobias, Editors, Interscience, New York (1963).
4. M. Y. Abyaneh and M. Fleischmann, *Trans. Inst. Metal Finishing*, **58**, 91 (1980).
5. M. Y. Abyaneh and M. Fleischmann, *J. Electroanal. Chem. Interfacial Electrochem.*, **119**, 197 (1981).
6. M. Y. Abyaneh and M. Fleischmann, *ibid.*, **119**, 187 (1981).
7. M. Y. Abyaneh, Ph.D. Thesis, Southampton University, 1980.
8. M. Y. Abyaneh and M. Fleischmann, *Electrochim. Acta*, **27**, 1513 (1982).
9. M. Avrami, *J. Chem. Phys.*, **7**, 1103 (1939); *ibid.*, **8**, 212 (1940); *ibid.*, **9**, 177 (1941).
10. M. Y. Abyaneh, E. Barendrecht, and H. Zeilmaker, In preparation.
11. N. Itoh, N. Yamazoe, and T. Seiyama, *Surface Technol.*, **5**, 27 (1977).
12. M. Y. Abyaneh, *Electrochim. Acta*, **27**, 1329 (1982).
13. G. Adzic, J. McBreen, and M. G. Chu, *This Journal*, **128**, 1691 (1981).
14. J. O'M. Bockris, Z. Nagy, and A. Damjanovic, *ibid.*, **119**, 285 (1972).
15. N. A. Hampson, G. A. Herdman, and R. Taylor, *J. Electroanal. Chem. Interfacial Electrochem.*, **25**, 9 (1970).
16. T. P. Dirkse and N. A. Hampson, *Electrochim. Acta*, **17**, 135 (1972); *ibid.*, **17**, 383 (1972); *ibid.*, **17**, 1113 (1972).